Optical Materials 72 (2017) 241–246

Contents lists available at ScienceDirect

Optical Materials

journal homepage: www.elsevier.com/locate/optmat

Invited Article

Fabrication of micron and submicron gratings by using plasma treatment on the curved polydimethylsiloxane surfaces

Jiangtao Yang [a, b, *], Jun Tang [a, b], Hao Guo [a, b], Wenyao Liu [a, b], Chong Shen [a, b], Jun Liu [a, b, **], Li Qin [a, b, ***]

[a] Science and Technology on Electronic Test & Measurement Laboratory (North University of China), Shanxi, 030051, China
[b] Key Laboratory of Instrumentation Science & Dynamic Measurement (North University of China), Ministry of Education, Shanxi, 030051, China

ARTICLE INFO

Article history:
Received 12 April 2017
Received in revised form
6 June 2017
Accepted 7 June 2017

Keywords:
Thin films
Wrinkled gratings
Oxygen plasma
Spectroscopy

ABSTRACT

Here, a simple and low-cost fabrication strategy to efficiently construct well-ordered micron and submicron gratings on polymeric substrates by oxygen plasma treatment is reported. The Polydimethylsiloxane (PDMS) substrate is prepared on the polyethylene (PET) by spin-coating method, then the curved PDMS-PET substrates are processed in oxygen plasma. After appropriate surface treatment time in plasma the curved substrates are flattened, and well-ordered wrinkling shape gratings are obtained, due to the mechanical buckling instability. It is also demonstrated that changing the curvature radius of PDMS-PET substrates and the time of plasma treatment, the period of the wrinkling patterns and the amplitude of grating also change accordingly. It is found the period of the wrinkling patterns increased with the radius of curvature; while the amplitude decreased with that. It also shows good optical performance in transmittance diffraction testing experiments. Thus the well-ordered grating approach may further develop portable and economical applications and offer a valuable method to fabricate other optical micro strain gauges devices.

© 2017 Elsevier B.V. All rights reserved.

1. Introduction

Folding structures are ubiquitous in the natural environment, such as human skin, dehydrated fruit skin and rolling hills, etc. Recently these folding structures have been imitated to fabricate nanostructure self-assembly templates [1,2], twisted liquid crystal displays [3], stretchable electrodes or interconnects [4,5], optical devices [6,7], microfluidic devices [8], thin film metrology [9–11], etc.

At present, there are two methods commonly used to fabricate the periodic structure, i.e. lithography and self-assembly technologies. However, lithography technology is relatively expensive, not suitable for the large scale production. In contrast, self-assembly method is low cost, and thus it is a commonly used method.

Polydimethylsiloxane (PDMS) is a commercially available clean room compatible type of elastic polymer material with awide range of applications, due to the low glass transition temperature, low surface energy, high transparency, excellent insulating performance and chemical stability performance. In most of the published research works, PDMS has been used as an elastomeric substrate. Several creative methods have been developed to improve its surface properties, including heating [13,14], mechanical stretching, compression [15–18], and chemical oxidation [12,20,21], which contribute to the formation of various layer on the surface. When the PDMS films are properly stretched and the residual stresses exceed the critical value, the PDMS wrinkles could be formed on the surface of the substrate. Using these techniques, various wrinkling patterns could been produced, including gratings [6], microlenses [7], checkerboard patterns [19], etc. Especially, the grating based on PDMS has good tunability and excellent diffraction effects in the visible light wave band. There are many feasible methods have been widely used to form uniform wrinkles of grating.

For example, Masashi Watanabe and Koujirou Mizukami [21] reported using a mixture of sulfuric acid and nitric acid on a

* Corresponding author. Science and Technology on Electronic Test & Measurement Laboratory (North University of China), Shanxi, 030051, China.
** Corresponding author. Science and Technology on Electronic Test & Measurement Laboratory (North University of China), Shanxi, 030051, China.
*** Corresponding author. Science and Technology on Electronic Test & Measurement Laboratory (North University of China), Shanxi, 030051, China.
E-mail addresses: yangjiangtao_nuc@163.com (J. Yang), liuj@nuc.edu.cn (J. Liu), qinli@nuc.edu.cn (L. Qin).

http://dx.doi.org/10.1016/j.optmat.2017.06.016
0925-3467/© 2017 Elsevier B.V. All rights reserved.

www.spm.com.cn

PDMS substrate formed wrinkles with a well-ordered stripe pattern. However, when the oxidation duration varies, the stripe patterns appear substantially different, and the required experimental high-temperature environment is difficult to control. Unlike chemical oxidation, oxygen plasma treatment is commonly used to create a stiff surface layer. Later, Cunjiang Yu et al. [6] reported a simple method to fabricate the tunable gratings on prestretched PDMS substrate by oxygen plasma treatment. In this paper, we propose a simple method to manufacture micron and submicron scale grating patterns on the curved PDMS surface by combining surface stress control and oxygen plasma treatment. And there are not any cracks on the grating patterns surface. After diffraction testing, the tunable elastic polymeric grating exhibites good tunability, and the self-formed grating could further serve as a strain sensors.

2. Experiment

The transparent PDMS substrates were prepared by casting the mixture of base and curing agent at the ratio of 10:1 by weight (Sylgard-184, Dow Corning); then, the mixture was degassed in a vacuum chamber and spin coated on a clean polyethylene (PET) substrate (~0.5 mm), then cured at 65 °C for 3 h. Finally, the obtained PET-PDMS sheets (~0.8 mm) were cut into 10 × 30 mm^2 and 10 × 50 mm^2 slabs.

Experimental schedule is listed in Fig. 1. Both ends of the PET-PDMS sheets are clamped by using a custom-made jig and applied prestress to obtain a symmetrical bending of the sheet; the L values are 0.5 cm and 2.5 cm, respectively, △L are 0.4 cm and 1 cm, r (radius of curvature of the center area) are 1.4 mm and 5.6 mm, respectively. The prestretched PET-PDMS specimens are treated by using oxidation plasma (PVA TePla ION Wave 10) with input power of 150 W and oxygen flow rate of 150 sccm; the reaction time is systematically set in the range of 60–540 s. After plasma treatment, the surface is capped with a glassy layer; when the sheet is released from the bending restriction, the strain mismatch between the hard coating and the polymer substrate leads to buckling of the surface glassy layer. In addition, we find that in the process of the grating fabrication, the period *d* and amplitude *A* are almost unchanged when the radius of curvature and plasma treatment time are controlled well and remain unchanged. As shown in Fig. 2, we carry out 50 experiments under the same conditions that the errors on period and amplitude are basically floating in 60 and 5 nm, respectively. Therefore, we conclude that the method has good repeatability.

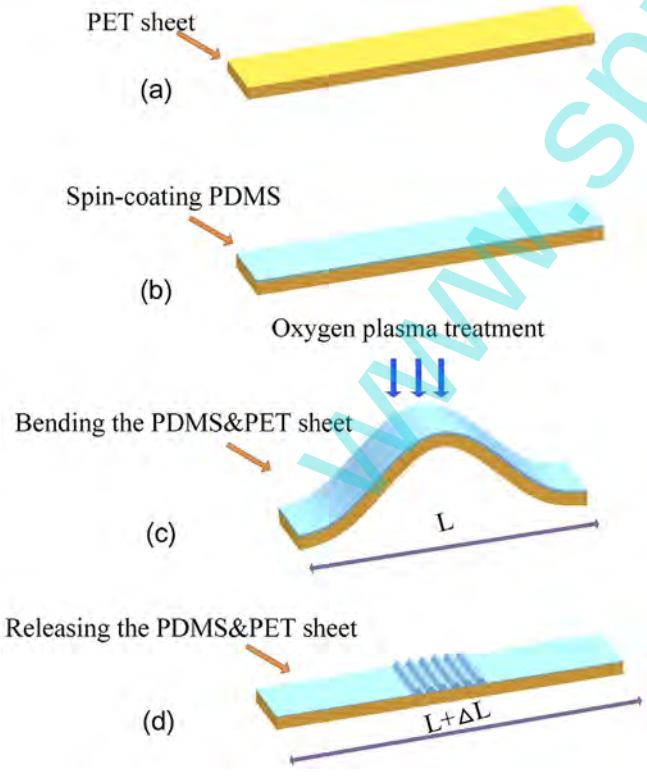

Fig. 1. Scheme of the fabrication of the micron and submicron gratings. (a) Prepared a polyethylene (PET) substrate (~0.5 mm); (b) The mixture of base and curing agent was spin coated on the PET substrate; (c) The prestretched PET-PDMS specimens were treated by using oxidation plasma (PVA TePla ION Wave 10); (d) Well-ordered wrinkles formed when the substrate was made flat again.

3. Results and discussions

3.1. Morphology

The surface morphology was analyzed by using atomic force microscopy (AFM; CSPM-5000, Benyuan) and laser scanning confocal microscopy (LEXT OLS4100, OLYMPUS). After the oxygen plasma treatment, the surface of PDMS became brittle. Notably, owing to the thermal expansion instability and the influence of the Poisson effect, the period and shape of the wrinkling patterns were difficult to control. Thus, in this work, the PDMS-PET sheets were bent and the stress was exerted very homogeneously, which is different from the study that stretching PDMS slab along a single planar direction [18].

Fig. 3(a) shows a PET-PDMS sheet (180 s, r = 1.4 mm) after releasing the strain from the oxygen plasma treated PET-PDMS sheet. The usable surface area of the film is the center area (about 1 cm long) where the curvature is relatively close. The diffraction wavelengths induced by the gratings could be modulated by deforming and bending the flexible substrates under the indoor light. The photograph of the colorful PDMS grating clearly shows that all different parts of the wrinkling pattern had diffraction peaks; these peaks were symmetrically distributed with respect to the center of the sheet. We attributed this phenomenon to the changing of the grating period. Well-ordered stripe patterns are observed via optical microscopy, as shown in Fig. 3(b). In order to demonstrate grating parameters clearly, the profile and side of this

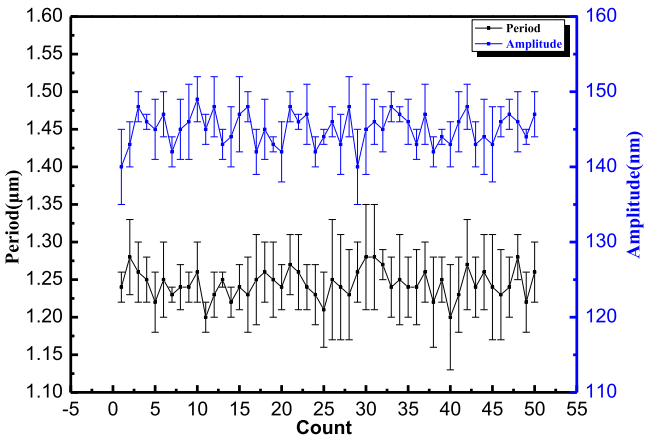

Fig. 2. The 50 experiments under the same conditions were carried out to test the repeatability of the grating. The error of period (left axis) and amplitude (right axis) is basically floating in 60 and 5 nm, respectively.

www.spm.com.cn

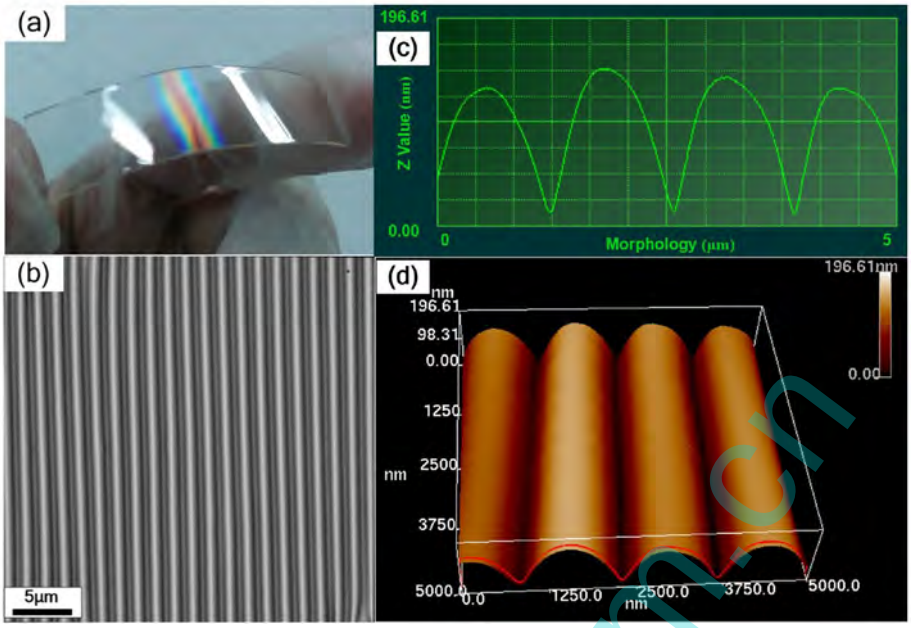

Fig. 3. (a) The PET-PDMS sheet (180 s, r = 1.4 mm) after releasing the strain from the oxygen plasma treated; (b) Well-ordered stripe patterns are observed via optical microscopy; (c) and (d) 3D atomic force microscopy reconstruction of well-ordered micron and submicron gratings on polymeric substrates by oxygen plasma treatment.

grating were also measured using AFM. As shown in Fig. 3(c) and (d), the period d and amplitude A were 1.25 μm and 0.15 μm, respectively.

As shown in Fig. 4, the thickness of stiff film approximately linearly increases with oxidation duration, and the period of the wrinkling shape grating is almost linearly proportional to the oxidation duration correspondingly. According to the linear buckling theory, the wrinkle period d and amplitude A of the wrinkling pattern can be theoretically expressed by the following equations [22]:

$$d = 2\pi h_f \left[\frac{E_f(1-\nu_s^2)}{3E_s\left(1-\nu_f^2\right)}\right]^{\frac{1}{3}} \quad (1)$$

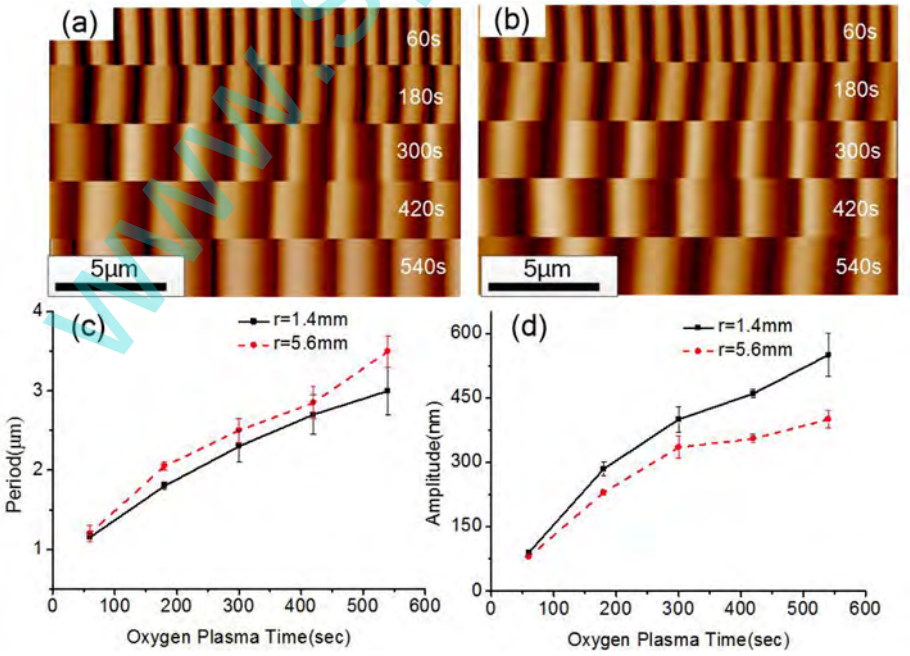

Fig. 4. Effect of treatment duration on period and amplitude of the wrinkling shape grating for different radius of curvature. Plane-view AFM images of stripe patterns with two different radius of curvature of the central region. (a) The radius of curvature is 1.4 mm for five rows, the plasma treatment times are 60 s, 180 s, 300 s, 420 s, 540 s from top to bottom. (b) The radius of curvature is 5.6 mm for five rows, the plasma treatment times are 60 s, 180 s, 300 s, 420 s, 540 s from top to bottom. (c) Period and (d) Amplitude of wrinkling shape grating vs different oxygen plasma treatment times and radius of curvature.

www.spn.com.cn

$$A = h_f\sqrt{\frac{\varepsilon_{pre}}{\varepsilon_c} - 1} \quad (2)$$

where E is Young's modulus and ν is Poisson's ratio. h is the thickness of the thin film (the subscripts 'f' and 's' denote to the top stiff layer and the bottom substrate, respectively). h_f is the thickness of the stiff thin film.

The critical strain ε_c can be theoretically expressed as:

$$\varepsilon_c = \frac{1}{4}\left[\frac{3E_s\left(1-\nu_f^2\right)}{E_f\left(1-\nu_s^2\right)}\right]^{\frac{2}{3}} \quad (3)$$

According to the equation, the periodicity and amplitude depend on the mechanical properties of hard coating and substrate, as well as the thickness of the stiff layer and prestrain of PDMS.

In our experiment, the periodicities of the wrinkling shape grating can be tuned by varying reaction time and radius of curvature. As shown in Fig. 4, as processing time is prolonged from 60 s to 540 s, the period and amplitude of the grating increased accordingly. In addition, the bending curvature (1/r) also is a key parameter to determine the prestrain of ε_{pre}. The smaller r values correspond to the larger ε_{pre} and A values. To verify the surface characteristics of the wrinkling shape grating patterns, the central area of the wrinkling shape grating is characterized via AFM. Fig. 4(c) and (d) show that curvatures of the central region are similar and periods of these stripe wrinkling patterns are in the range of 1.1–3.0 μm and 1.2–3.5 μm, and amplitudes are in the range of 90–550 nm and 80–400 nm, corresponding to the two different initial radius of curvature of 1.4 mm and 5.6 mm, respectively. Thus, the change of period was generally in good agreement with the theoretical prediction of Eq. (1). The wrinkle period was almost linearly proportional to the oxidation duration, as the thickness of the stiff film increased approximately linearly with the oxidation duration.

Moreover, in order to show the distribution of the grating, AFM was used to scan five samples, as shown in Fig. 5. The oxygen plasma treatment time is 540 s and the radius of curvature is 1.4 mm, 2.4 mm, 3.5 mm, 4.5 mm, 5.6 mm in turn, respectively. We also carried out 10 groups of data acquisition for every sample. It is observed that the grating period and amplitude present gradient distribution. The results showed that the periodicities of wrinkling patterns increased with the radius of curvature, while the amplitude showed the opposite trend.

3.2. The diffraction properties of wrinkling shape grating

Due to the good transparency for visible light, PDMS can be employed as a light-coupling mask for photolithography or the realization of optical waveguide systems. The tunable diffractive grating [6] made of PDMS showed great performance in the diffraction tests. To validate the well-ordered buckling structure of the grating sample created by this method, optical transmittance diffraction tests are conducted.

The law of diffraction can be theoretically expressed by the basic grating equation:

$$d(\sin\theta_i + \sin\theta_k) = k\lambda \quad (4)$$

where θ_i and θ_k are the angle of incidence and the diffraction order kth, respectively, can be measured from the grating surface normal; d refers to the period of the grating, and λ is the wavelength of the incident light. Moreover, to obtain a high grating resolvance in the visible light range, submicron scale period of the wrinkling shape grating is desired.

A schematic of the experimental setup is shown in Fig. 6(a). Hold the slit up to a source of light (xenon lamp), make the grating was irradiated vertically by light, while a spectrometer (AvaSpec-2048 × 14, Avantes) is placed at the angle of $\theta_k = 24°$ to detect the transmitted light. As there is an overlap between the second and the third diffraction orders, the first diffraction order was selected for testing. In this experiment, as the angles of $\theta_i = 0°$ and $\theta_k = 24°$ were fixed, $k\lambda/d$ could be considered constant. When the wrinkling shape grating is stretched, the period is increased, and the detected wavelength of the first-order diffraction light at θ_k is increased accordingly.

As shown in Fig. 6(b), the tested sample had been previously treated with oxygen plasma for 60 s and the radius of curvature of r = 1.4 mm, exhibiting a well-ordered stripe pattern on the surface. Fig. 6(b) shows that the average wavelength λ and amplitude A of the measured sample are 1.1 μm and 90 nm, respectively.

The value of strain is related to the ratio of curing agent and PDMS base. In order to ensure that there is no cracks when the grating is stretched, we measured a strain up to 10%. When the strain applied on the grating varied from 0 to 10%, the minimum and the maximum fitted peak wavelength of the first-order transmittance diffraction light received by the spectrometer were 452 nm and 507 nm, respectively, as shown in Fig. 6(c) and (d). The peak wavelength was plotted in Fig. 6(d). Thus, the results showed that the peak wavelength of the first-order diffraction increased

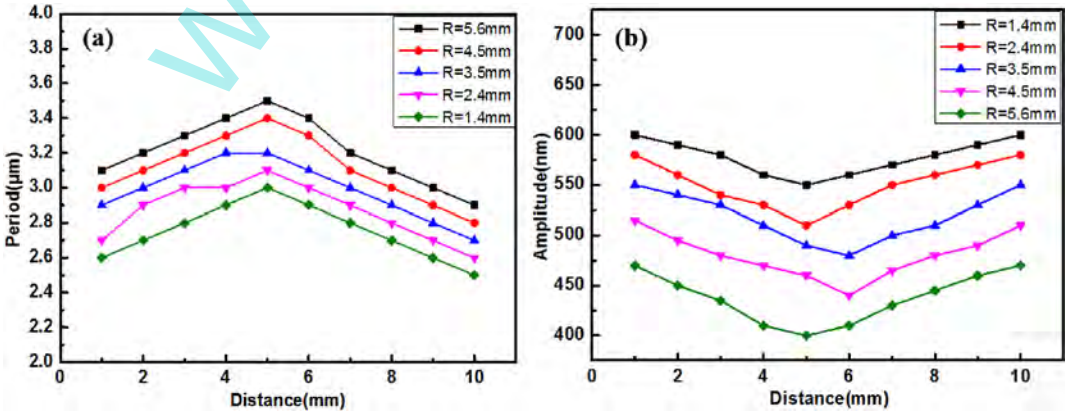

Fig. 5. In order to show the distribution of the grating, atomic force microscopy was used to scan five samples. The oxygen plasma treatment time is 540 s and the radius of curvature is 1.4 mm, 2.4 mm, 3.5 mm, 4.5 mm, 5.6 mm in turn, respectively. (a) The overall distribution of the wrinkle period and the periodicities increased with the radius of curvature. (b) The overall distribution of wrinkle amplitude and the amplitude decreased with the radius of curvature.

www.spm.com.cn

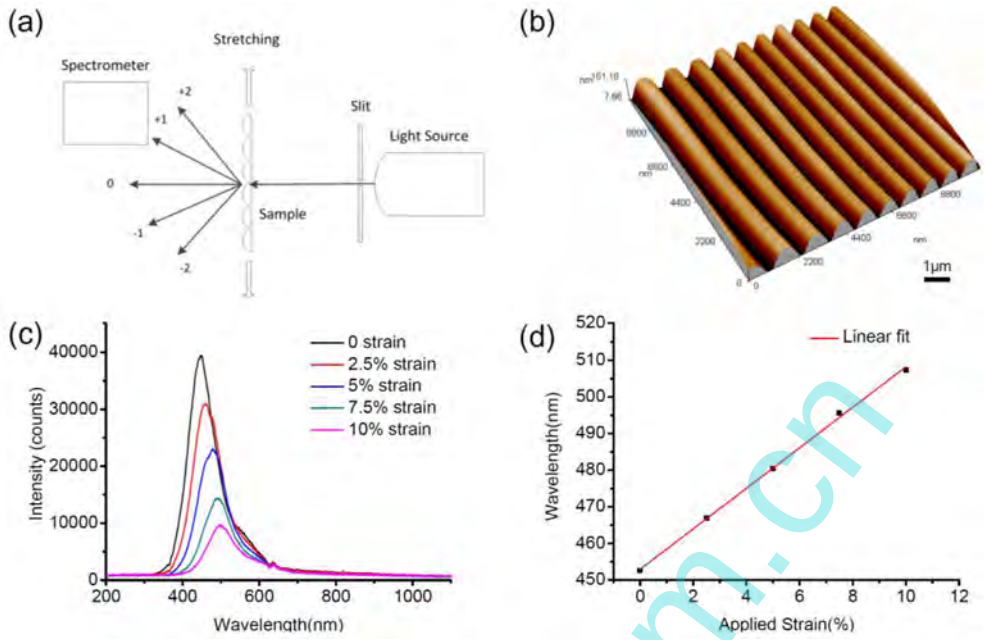

Fig. 6. The test of the diffraction properties of tunable diffractive grating. (a) Schematic experimental procedure to measure the diffraction grating. (b) AFM image of the sample that oxygen plasma for 60 s and the radius of curvature of r = 1.4 mm. (c) Peak wavelength shift of received first-order diffracted light. (d) The peak wavelength of the diffraction light increases linearly with the applied strain, ranging from 452 to 507 nm.

linearly with the applied strain.

4. Conclusions

A facile method to fabricate well-ordered and crack-free wrinkling patterns was presented. The oxygen plasma treatment of a PET-PDMS substrate produced well-ordered stripe patterns on the surface of the polymer sheet by release of the mechanical strain. The period and amplitude of the wrinkling shape grating could be well controlled by varying the radius of curvature of the curved sheet. And the period increased with the radius of curvature; while the amplitude decreased with that. Thus, this approach can be potentially applied to create gradient wrinkling patterns. In addition, the ordered buckling structure could be used as a tunable diffractive grating. Moreover, the wavelength shift was proportional to the applied strain or grating period, revealing the good periodicity of the wrinkling pattern. The application of self-formed wrinkles in optical devices, microfluids and nanoimprint lithography is very promising.

Author contributions

Jiangtao Yang and Jun Tang contributed equally to this work. Hao Guo, Wenyao Liu and Chong Shen prepared the samples and performed the AFM measurements. Jun Liu and Li Qin offered helpful discussion in the study. All authors reviewed the manuscript.

Funding sources

This work was supported by the National Natural Science Foundation of China, [grant numbers 51225504, 61127008, 61571405, 61603353].

Notes

The authors declare no competing financial interest.

Acknowledgments

We acknowledge the financial support from the Natural Science Foundation of China (51225504, 61127008, 61571405 and 61603353), program for the top young academic leaders of higher learning Institutions of Shanxi.

References

[1] A. Schweikart, N. Pazos-Pérez, R.A. Alvarez-Puebla, A. Fery, Controlling inter-nanoparticle coupling by wrinkle-assisted assembly, Soft Matter 7 (2011) 4093–4100.
[2] W.Q. Wan, W. Qiao, W.B. Huang, M. Zhu, Z.B. Fang, D.L. Pu, Y. Ye, Y.H. Liu, L.S. Chen, Efficient fabrication method of nano-grating for 3D holographic display with full parallax views, Opt. Express 24 (2016) 6203–6212.
[3] T. Ohzono, H. Monobe, R. Yamaguchi, Y. Shimizu, H. Yokoyama, Dynamics of surface memory effect in liquid crystal alignment on reconfigurable micro-wrinkles, Appl. Phys. Lett. 95 (2009), 014101.
[4] D.Y. Khang, H. Jiang, Y. Huang, J.A. Rogers, A stretchable form of single-crystal silicon for high-performance electronics on rubber substrates, Science 311 (2006) 208–212.
[5] D.H. Kim, J.H. Ahn, W.M. Choi, H.S. Kim, T.H. Kim, J. Song, Y.Y. Huang, Z. Liu, C. Lu, J.A. Rogers, Stretchable and foldable silicon integrated circuits, Science 320 (2008) 507–511.
[6] C. Yu, K. O'Brien, Y.-H. Zhang, H. Yu, H. Jiang, Tunable optical gratings based on buckled nanoscale thin films on transparent elastomeric substrates, Appl. Phys. Lett. 96 (2010), 041111.
[7] E.P. Chan, A.J. Crosby, Fabricating microlens arrays by surface wrinkling, Adv. Mater 18 (2006) 3238–3242.
[8] H.S. Kim, A.J. Crosby, Solvent-responsive surface via wrinkling instability, Adv. Mater 23 (2011) 4188–4192.
[9] C.S. WAN, T.K. Gaylord, M.S. Bakir, RCWA-EIS method for interlayer grating coupling, Appl. Opt. 55 (2016) 5900–5908.
[10] C.M. Stafford, C. Harrison, K.L. Beers, A. Karim, E.J. Amis, M.R. Vanlandingham, H.C. Kim, W. Volksen, R.D. Miller, E.E. Simonyi, A buckling-based metrology for measuring the elastic moduli of polymeric thin films, Nat. Mater 3 (2004) 545–550.
[11] D. Tahk, H.H. Lee, D.Y. Khang, Elastic moduli of organic electronic materials by the buckling method, Macromolecules 42 (2009) 7079–7083.
[12] A.J. Nolte, M.F. Rubner, R.E. Cohen, Determining the Young's modulus of polyelectrolyte multilayer films via stress-induced mechanical buckling instabilities, Macromolecules 38 (2005) 5367–5370.
[13] P.J. Yoo, K.Y. Suh, S.Y. Park, H.H. Lee, Physical self-assembly of microstructures by anisotropic buckling, Adv. Mater 14 (2002) 1383–1387.
[14] P.J. Yoo, H.H. Lee, Complex pattern formation by adhesion-controlled

www.sm.com.cn

anisotropic wrinkling, Langmuir 24 (2008) 6897–6902.
[15] P.C. Lin, S. Yang, Spontaneous formation of one-dimensional ripples in transit to highly ordered two-dimensional herringbone structures through sequential and unequal biaxial mechanical stretching, Appl. Phys. Lett. 90 (2007), 241903.
[16] Y. Xuan, X. Guo, Y. Cui, C. Yuan, H. Ge, B. Cui, Y. Chen, Crack-free controlled wrinkling of a bilayer film with a gradient interface, Soft Matter 8 (2012) 9603–9609.
[17] P. Kim, Y. Hu, J. Alvarenga, M. Kolle, Z. Suo, J. Aizenberg, Rational design of mechano-responsive optical materials by fine tuning the evolution of strain-dependent wrinkling patterns, Adv. Opt. Mater 1 (2013) 381–388.
[18] K.U. Claussen, M. Tebbe, R. Giesa, A. Schweikart, A. Fery, H.W. Schmidt, Towards tailored topography: facile preparation of surface-wrinkled gradient poly (dimethyl siloxane) with continuously changing wavelength, RSC Adv. 2 (2012) 10185–10188.
[19] T.K. Shih, J.R. Ho, C.F. Chen, W.T. Whang, C.C. Chen, Topographic control on silicone surface using chemical oxidization method, Appl. Surf. Sci. 253 (2007) 9381–9386.
[20] J.H. Wang, C.F. Chen, J.R. Ho, T.K. Shih, C.C. Chen, W.T. Whang, J.Y. Yang, One-step fabrication of surface-relief diffusers by stress-induced undulations on elastomer, Opt. Laser Technol. 41 (2009) 804–808.
[21] M. Watanabe, K. Mizukami, Well-ordered wrinkling patterns on chemically oxidized poly(dimethylsiloxane) surfaces, Macromolecules 45 (2012) 7128–7134.
[22] H. Jiang, D.Y. Khang, J. Song, Y. Sun, Y. Huang, J.A. Rogers, Finite deformation mechanics in buckled thin films on compliant supports, Proc. Natl. Acad. Sci. U. S. A. 104 (2007) 15607–15612.

www.spm.com.cn